

QUANTITATIVE ANALYSIS OF THE BINDING STRENGTH AND
ADSORPTION CAPACITY OF ZINC OXIDE NANOPARTICLES ONTO
UNMODIFIED AND MODIFIED COTTON FIBER

A thesis presented to the faculty of the Graduate School of Western
Carolina University in partial fulfillment of the requirements for the degree
of Master of Science in Chemistry.

By

Stephen Robert Printz

Advisor: Dr. Carmen Huffman
Associate Professor of Chemistry
Department of Chemistry & Physics

Committee Members: Dr. David Evanoff, Chemistry & Physics
Dr. Channa De Silva, Chemistry & Physics

July 2016

ACKNOWLEDGMENTS

I'd like to thank Western Carolina University for providing such an excellent environment for my education. I'd like to thank the members of my thesis committee, Dr. Channa De Silva and Dr. David Evanoff, for their time and for their sound advice, whether in the classroom, the lab, an office, or a conference room. Finally, I'd like to thank Dr. Carmen Huffman for always being willing to help even when I was too stubborn to ask for it, and for being the one who finally told me why things happened, and then showed me the math to prove it.

TABLE OF CONTENTS

LIST OF TABLES	iv
LIST OF FIGURES	v
ABSTRACT	vi
CHAPTER 1: INTRODUCTION	1
1.1 Motivation	1
1.2 Goals	2
1.3 Background	2
1.3.1 Adsorption	2
1.3.2 Fiber	4
CHAPTER 2: EXPERIMENTAL	9
2.1 Materials	9
2.2 Zinc Oxide Nanoparticle Synthesis and Characterization	9
2.3 Textile Preparation, Modification, and Characterization	11
2.4 Adsorption of Zinc Oxide Nanoparticles to Textiles	12
2.4.1 Kinetics of Adsorption	12
2.4.2 Adsorption Isotherms	12
2.4.3 Scanning Electron Microscopy	13
2.4.4 Wash Durability	14
CHAPTER 3: RESULTS AND DISCUSSION	15
3.1 Nanoparticle Characterization	15
3.1.1 Crystal Size	15
3.1.2 Hydrodynamic Diameter	17
3.2 Fabric Modification	18
3.3 Adsorption	23
3.3.1 Adsorption Kinetics	23
3.3.2 Adsorption Isotherms	24
3.3.3 Energy Dispersive X-Ray Spectra of Cloth with Nanoparticles	29
3.4 Wash Durability	33
CHAPTER 4: CONCLUSION	35
REFERENCES	36

LIST OF TABLES

Table 1.	Parameters used in the Scherrer equation and the crystal size of powder zinc oxide nanoparticles.	16
Table 2.	Hydrodynamic diameters and polydispersity indices of zinc oxide nanoparticles suspended in water.	18
Table 3.	Percent mass of components on modified cloth. The uncertainties in percentages are between 0.2 and 0.3% as determined by error propagation.	22
Table 4.	Approximate moles of citric acid, α -CD, and β -CD per square centimeter of cloth.	23
Table 5.	Decrease in nanoparticle concentration over time.	24
Table 6.	Adsorption capacities (Q_o in mg ZnO/g cloth), relative binding strengths (b in ppm ⁻¹) and root mean square error (RMSE) from the fit to the Langmuir equation for each type of cloth that was tested.	29
Table 7.	Elemental weight percentages for each type of cloth. Uncertainties are between 0.2 and 0.3%.	33

LIST OF FIGURES

Figure 1.	Molecular structure of cellulose chain.	5
Figure 2.	Intramolecular and intermolecular hydrogen bonding in Cellulose I.	6
Figure 3.	Intramolecular and intermolecular hydrogen bonding in Cellulose II.	7
Figure 4.	Chemical structures of α - and β - cyclodextrin.	7
Figure 5.	Structure of cellulose monomer connected to α - or β -cyclodextrin molecule (n= 6 or 7, respectively) via a citric acid linker.	8
Figure 6.	X-ray powder diffraction spectrum of zinc oxide nanoparticles. .	15
Figure 7.	SEM image of zinc oxide nanoparticles.	17
Figure 8.	Hydrodynamic diameter distribution of zinc oxide nanoparticles.	18
Figure 9.	Change in color of mercerized cotton cloth (a) before and (b) after addition of phenol red.	19
Figure 10.	Infrared spectrum of citric acid, α -CD, unmodified mercerized/bleached cloth, and α -CD modified mercerized/bleached cloth.	20
Figure 11.	Infrared spectrum of citric acid, β -CD, unmodified mercerized/bleached cloth, and β -CD modified mercerized/bleached cloth.	21
Figure 12.	Percentage increase in cloth mass after modification with citric acid alone (green), and citric acid with α -CD (blue) or β -CD (orange).	22
Figure 13.	ZnO concentration over time in the presence of cotton cloth samples.	24
Figure 14.	Adsorption isotherm for unmodified cloths.	26
Figure 15.	Adsorption isotherms for mercerized cloth.	26
Figure 16.	Adsorption isotherm for bleached cloth.	27
Figure 17.	Adsorption isotherm for unbleached cloth.	27
Figure 18.	SEM image of zinc oxide nanoparticles bound onto unmodified cloth.	30
Figure 19.	EDX map of cotton fiber highlighting (b) carbon (red), (c) oxygen (green), and (d) zinc (blue).	31
Figure 20.	SEM image of (a) unmodified, (b) α -CD modified, and (c) β -CD modified mercerized/bleached cloth. White specks are clusters of zinc oxide nanoparticles.	32
Figure 21.	Elemental analysis of unmodified (blue), α -CD modified (orange), and β -CD modified (gray) cloth.	33
Figure 22.	Chart of the change in coverage with consecutive washes.	34

ABSTRACT

QUANTITATIVE ANALYSIS OF THE BINDING STRENGTH AND ADSORPTION CAPACITY OF ZINC OXIDE NANOPARTICLES ONTO UNMODIFIED AND MODIFIED COTTON FIBER

Stephen Robert Printz, Masters of Science in Chemistry

Western Carolina University (July 2016)

Advisor: Dr. Carmen Huffman

Risk of bacterial infection is always a concern in hospitals, so it is important to find ways to minimize this risk. One method for reducing the risk of infection is by using textiles with antimicrobial properties. Zinc oxide nanoparticles have antimicrobial properties, and can be adsorbed onto cotton fibers to pass these properties to the cloth. However, the binding of the zinc oxide nanoparticles to cotton is weak, so the particles desorb from the cloth after repeated washings. The goal of this project was to quantify the binding strength of zinc oxide nanoparticles onto different types of cotton fiber. The cotton was modified by grafting cyclodextrin onto it with citric acid as a crosslinking agent. Adsorption was tested with desized, unbleached cotton print cloth; desized, bleached cotton print cloth; and desized, bleached, mercerized cotton print cloth. As expected, adsorption to unmodified cloth was poor. Unbleached cloth had the highest adsorption capacity ($Q_0 = 22 \pm 4$ mg ZnO/g cloth), and bleached cloth had the lowest adsorption capacity ($Q_0 = 17 \pm 4$ mg ZnO/g cloth). Mercerized cloth had the lowest strength ($b = 0.010 \pm 0.003$ ppm⁻¹), and bleached cloth had the highest binding strength ($b = 0.04 \pm 0.01$ ppm⁻¹). Modification with α -cyclodextrin increased adsorption capacity over unmodified cloth by 61, 80, and 70 % for mercerized/bleached cloth, bleached cloth, and unbleached cloth, respectively, and increased b by 1601, 126, and 90 %

respectively. Modification with β -cyclodextrin increased adsorption capacities by 80, 94, and 112 %, respectively, and increased b by 2027, 427, and 46 %. As a result, β -CD modified unbleached cloth had the highest adsorption capacity and one of the lowest binding strengths. However, β -cyclodextrin modified mercerized cloth has both a high adsorption capacity and a high binding strength, and would likely be the best candidate for use in antimicrobial textiles.

CHAPTER 1: INTRODUCTION

1.1 Motivation

The risk of infection is an ever present threat in hospitals. An infection that develops after 48 hours of hospitalization which was not present or incubating before admission is called a hospital-acquired infection (HAI).¹ There are over 1.7 million reported cases of HAIs in the US every year, costing approximately \$9.8 billion.¹ Not only do they increase medical costs, they also increase length of stay, complication rates, and overall morbidity and mortality in hospitals across the nation.¹ As much as 84 % of HAIs are caused by 10 common pathogens, with up to 16 % being caused by multidrug-resistant pathogens.² Hospitals try to minimize the risk of infection through systematic implementation of cleaning protocols, including hand washing, use of alcohol-based gels, screening and surveillance cultures, isolation protocols, strict cleaning regimens for room turnovers, lowering bed occupancy, no white coat or bare below the elbows policies, and encouraging more judicious use of antibiotics.¹ Despite these efforts, the risk still remains fairly high. Even with the rigorous cleaning protocols in place, laundering of hospital textiles tends to focus on removing stains, often leaving them clean to the eye, but not necessarily sterile.³ Bacteria can survive for weeks on hospital textiles, during which time they can be transported to new potential hosts.⁴

However, it might be possible to passively reduce the risk of infection through the use of antimicrobial surfaces. Advances in nanoparticle chemistry have caused a shift in clothing research toward the modification of fibers to allow for new and unusual properties. Zinc oxide (ZnO) nanoparticles are well known for their broadband UV absorption and photosensitivity.⁵⁻⁷ Photosensitive materials react when they absorb photons, which can cause antimicrobial effects.⁷⁻⁹ ZnO nanoparticles can absorb UV or visible light and, through radical formation, produce H_2O_2 , which can kill bacteria by penetrating their cell walls.⁷

This antimicrobial activity can occur when the nanoparticles are adsorbed onto cotton fibers.⁹ However, crystalline ZnO nanoparticles do not adsorb strongly to cotton fibers, and are quickly removed during washing; this causes the properties to wane after successive washes.⁹

1.2 Goals

The goal of this study was to quantitatively characterize the adsorptivity (i.e. the binding strength and adsorption capacity) of ZnO nanoparticles onto a variety of cotton fabrics.

Adsorption to three different types of cotton print cloth was tested to determine the effects of various processing methods on the adsorptivity: unbleached, bleached, and mercerized and bleached. Some fabrics were modified by grafting cyclodextrin onto their surfaces. We hypothesize that the modification will increase adsorptivity because the cyclodextrin provides a hydroxyl-rich environment which should encourage nanoparticle binding.

1.3 Background

1.3.1 Adsorption

Adsorption is the process by which a surface-active substance interacts with a large adsorbing surface. When a dilute solution of the surface-active substance, or adsorbate, comes in contact with the surface, called the adsorbent, the substance becomes bound to the surface at specific locations, called binding sites.¹⁰ The process of adsorption is viewed as an equilibrium, as shown in Equation 1. On one side of the equation, there is unbound adsorbate in solution and empty binding sites on the adsorbent surface; on the other, there is bound adsorbate.¹⁰



An adsorption isotherm is a plot of surface coverage, q_e , the ratio of bound adsorbate to adsorbent, versus the equilibrium concentration of the free adsorbate, C_e . Experimental data can often be fit using the Langmuir Equation,

$$q_e = \frac{Q_0 b C_e}{1 + b C_e} \quad (2)$$

where Q_0 is the maximum possible surface coverage, also called the adsorption capacity, and b is the Langmuir constant, which represents the adsorption equilibrium constant. The Langmuir model assumes that the adsorbate behaves like an ideal gas under isothermal conditions. The adsorbent is viewed as an ideal solid surface that is a perfectly flat, homogeneous plane. The surface of the adsorbent is composed of distinct, but equivalent sites where a single molecule of adsorbate can bind to an immobile state. The model also assumes that adsorbate molecules bound on adjacent sites do not interact with each other.¹⁰ Even if these assumptions are not appropriate, the Langmuir model is routinely used for fitting adsorption data with good results.

The Langmuir model can be used to describe adsorption via either physisorption or chemisorption.¹¹ Physisorption results from van der Waals forces, while chemisorption requires the transfer or sharing of electrons between the adsorbent and the adsorbate. As a result, chemisorption usually results in a much stronger binding.¹²

The binding strength is typically reported in terms of enthalpy (ΔH), with negative (exothermic) values indicating strong bonding. The determination of these values requires temperature-dependent measurements. Enthalpy is related to the Gibbs energy of adsorption (ΔG) through the following equation

$$\Delta G = \Delta H + T\Delta S \quad (3)$$

where T is the absolute temperature (kelvin) and ΔS is the change in entropy for the

adsorption process. If the differences in changes in entropy from experiment to experiment are considered negligible (a rudimentary assumption), then the enthalpy is proportional to ΔG . The Langmuir constant, b , can be used to calculate ΔG of the adsorption process:

$$\Delta G = -RT \ln(b) \quad (4)$$

where R is the ideal gas constant ($8.314 \times 10^{-3} \text{ kJ mol}^{-1} \text{ K}^{-1}$). Some controversy still exists concerning a proper method for using Equation 4 due to the fact that b is not unitless.^{13,14} In most cases, b is given in units of 1/molarity. However, expressing nanoparticle concentrations in molarity poses significant challenges when nanoparticle size is not adequately defined, so ppm is a more common unit. As such, ΔG can not be directly calculated. However, since ΔG is inversely proportional to b , the Langmuir constant can be used as a measure of relative binding strength (abiding the assumption that ΔS does not vary is valid, which may or may not be the case).

1.3.2 Fiber

Cellulose is the primary component of cotton. Cellulose is a macromolecule made up of D-glucopyranose ring units linked by β -1,4 glycosidic bonds as shown in Figure 1.¹⁵ The glycosidic bonds cause cellulose to form long, linear chains, alternating 180° along the chain axis. Each glucopyranose monomer has three reactive hydroxyl groups, at C2, C3, and C6. While ZnO nanoparticles have been shown to mechanically bind to the surface of cotton fabric,¹⁶ the hydroxyl groups are the most likely binding sites due to their polarity. We hypothesize that the more hydroxyl groups present and the greater their accessibility, the greater the nanoparticle binding strength and adsorption capacity will be. The orientation of the C2, C3, and C6 hydroxyl groups causes cellulose molecules to form intra- and inter-molecular hydrogen bonds. The manner in which this hydrogen bonding occurs determines

the overall 3-D structure of the macromolecule.^{15,17}

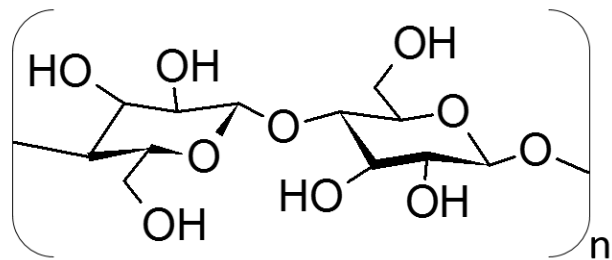


Figure 1. Molecular structure of cellulose chain.

In its natural state, called Cellulose I, hydrogen bonding occurs between the C6 hydroxyl of one unit in the chain and the C2 hydroxyl of its neighbor, while the C3 hydroxyl bonds with the ether oxygen in the neighbor, as shown in Figure 2. The intramolecular hydrogen bonding, with the β links, causes the rigidity of cellulose molecules, and leads to a high tendency to form fibrillar structures.¹⁵ Intermolecular hydrogen bonding can occur between adjacent macromolecules, primarily between the oxygen of the C3 hydroxyl and the hydroxyl of the C6 in an adjacent chain, as shown in Figure 2.¹⁵ The hydrogen bonding causes parallel chains to form into fibers 100 nm long and 1.5-3.5 nm wide. These fibers form 10-30 nm wide bundles called microfibrils, which in turn form microfibrillar bands that can be hundreds of nanometers long.¹⁵ This pattern of bonding causes the cellulose to arrange itself in a sheet-like structure, with the sheets held together by van der Waals forces.

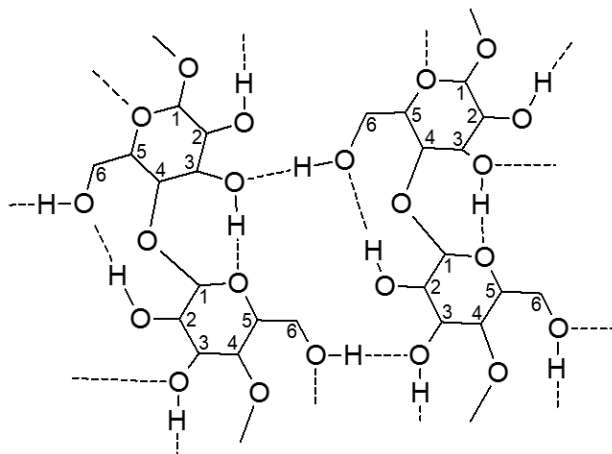


Figure 2. Intramolecular and intermolecular hydrogen bonding in Cellulose I.

Cotton fibers under tension can be treated with an alkali solution, most commonly sodium hydroxide, to cause the sheets which make it up to break apart. This allows for the formation of new hydrogen bonds.¹⁷ This process, called mercerization, changes the Cellulose I into Cellulose II. In Cellulose II, intermolecular hydrogen bonding occurs between the hydroxyl of a C6 in one chain and the hydroxyl of a C2 in an adjacent chain, as shown in Figure ??.

The new orientations created during the mercerization process allow for bonding between different planes in the supramolecular structure, which causes the fibers to swell.¹⁸ The mercerized fibers therefore have more surface area than the unmercerized fibers. The increased surface area should correspond to an increase in the number of accessible hydroxyl groups, and therefore an increased number of binding sites available for nanoparticles, and greater adsorption capacity. This is observed in the dyeing process. Mercerized cloth absorbs more dye and is resistant to fading during washing, suggesting a greater adsorption capacity and binding strength for dyes.

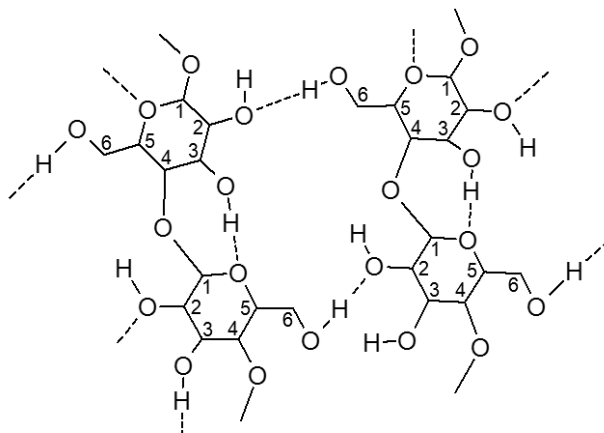


Figure 3. Intramolecular and intermolecular hydrogen bonding in Cellulose II.

The bleaching process oxidizes surface hydroxyl groups to carboxylic acids,¹⁹ which can also act as binding sites for zinc oxide nanoparticles because of their polarity. They are more polar than hydroxyl groups, and as such they will interact more strongly with the adsorbate molecules. So, the bleached fabric should have a stronger nanoparticle binding affinity than the unbleached fabric.

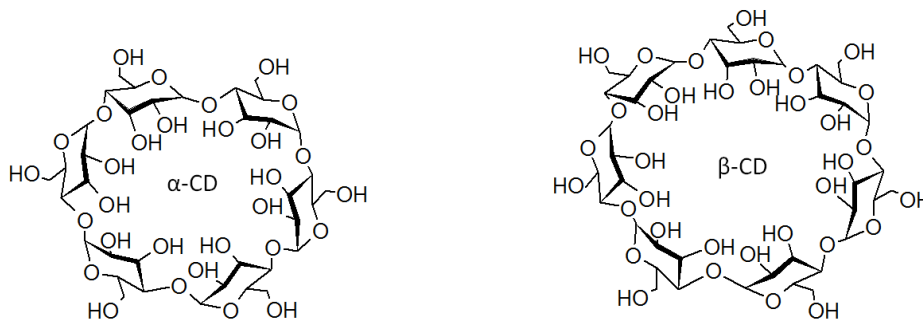


Figure 4. Chemical structures of α - and β - cyclodextrin.

Cyclodextrins are macrocyclic oligosaccharides made from glucopyranose units linked by α -(1,4)-glycosidic bonds. α -cyclodextrin contains six glucopyranose units and β -cyclodextrin contains seven units, which form an elongated toroid structure.²⁰ The structures of α - and β -cyclodextrin are shown in Figure 4. Grafting of the cyclodextrins onto cellulose can be achieved by using citric acid as a cross-linking agent, as shown in Figure 5.^{8,20,21} It is hoped

that the cyclodextrins will provide a hydroxyl-rich environment that is more favorable to adsorption. Since the β -cyclodextrin contains more glucopyranose units, it is expected to increase adsorptivity more than α -cyclodextrin.

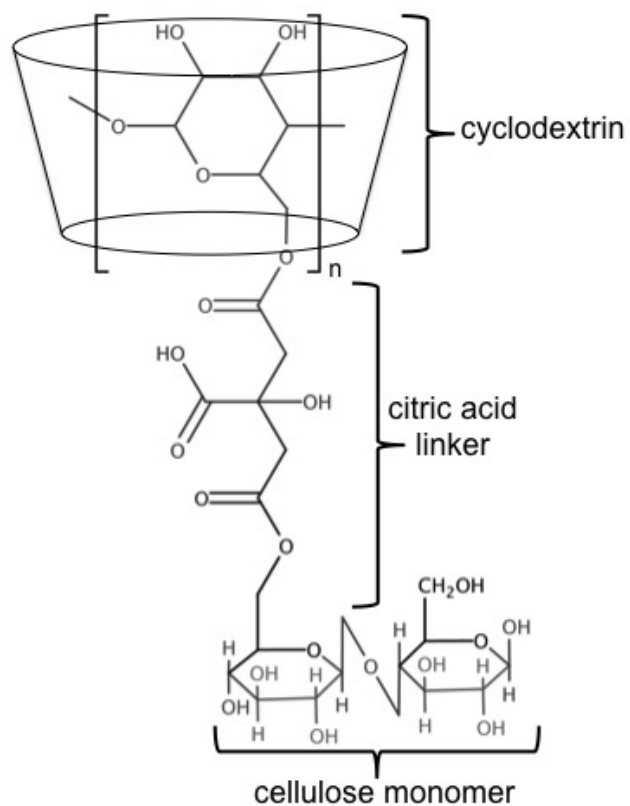


Figure 5. Structure of cellulose monomer connected to α - or β -cyclodextrin molecule ($n= 6$ or 7 , respectively) via a citric acid linker.

CHAPTER 2: EXPERIMENTAL

2.1 Materials

Zinc acetate dihydrate (>98% pure) was purchased from Acros Organics. Methanol (reagent grade), citric acid (lab grade), nitric acid (certified ACS Plus grade), and zinc nitrate hexahydrate (reagent grade) were purchased from Fisher Scientific. Sodium hydroxide (>98% pure) was purchased from Sigma-Aldrich. Sodium phosphate dibasic (ACS reagent grade) was purchased from Kodak. α -cyclodextrin was purchased from Avocado Research Chemicals, Inc. β -cyclodextrin was purchased from Alfa Aesar, Inc. Unbleached cotton print cloth (400u), bleached cotton print cloth (400), and mercerized, bleached cotton print cloth (400m) were purchased from Test Fabrics, Inc. All compounds were used without further purification or modification unless noted elsewhere. All solutions, suspensions, and washing baths were prepared using ultra pure water from either a Millipore MilliQ Gradient or Barnstead Ultrapure water filtration system with a resistivity of $\geq 18\text{M}\Omega\text{cm}$. Sonication of suspensions was carried out in a Fisher Scientific FS 30H bath, and centrifugation was carried out in a Sorvall RC5Cplus. Samples containing nanoparticle suspension and submerged cloth were spun on a Thermo-Scientific tube revolver. Drying was carried out in a VWR 1305U oven.

2.2 Zinc Oxide Nanoparticle Synthesis and Characterization

Zinc oxide nanoparticles were synthesized using a method described previously.²² First, 0.0200 mol of zinc acetate dihydrate ($\text{Zn}(\text{O}_2\text{CCH}_3)_2 \cdot 2\text{H}_2\text{O}$) was added to 100 mL of methanol and stirred overnight. Then, 15 mL of 3 M aqueous sodium hydroxide (NaOH) was added dropwise under vigorous stirring forming a white suspension, which was stirred for 12 h. The final pH of the reaction mixture was 13. The solid particles were separated by centrifugation at 4500 rpm for 15 min. The precipitate was washed twice with 50 mL of methanol and

centrifuged under the same conditions, and then the particles were dried for 12 h at 100 °C. The dried product was ground into a fine powder with a pestle and mortar and stored in a clean scintillation vial. Synthesis had a 93% yield. Zinc oxide nanoparticle suspensions were prepared by mass and the concentrations of these suspensions are expressed in ppm, which is μg of nanoparticles per gram of suspension. When nitric acid was to suspensions or cloth to digest the nanoparticles, the Zn(II) concentration was determined and converted to the ZnO concentration using molar masses. Concentrations of these solutions are reported as the mass of ZnO per mass of solution in ppm.

Nanoparticle crystal size was determined using X-ray powder diffraction spectroscopy. X-ray powder diffraction spectra were collected using a desktop X-ray diffractometer Mini-Flex⁺, with a Co-K α ($\lambda = 1.78899 \text{ \AA}$) radiation with a scan speed of $0.5 \text{ }^\circ\text{min}^{-1}$. Diffraction spectra were collected from $2\theta = 3^\circ$ to $2\theta = 80^\circ$. The X-ray source was set to a power of 30 kV and a current of 15 mA. Data were converted to a Cu lamp reference scale and analyzed using Materials Data Jade 7 software.

Scanning electron microscopy was performed to confirm nanoparticle size and to observe the shape and uniformity of the particles. Images were acquired at the Clemson Advanced Materials Research Laboratory under the direction of Mr. George Wetzel using the S4800 instrument. A few drops of zinc oxide nanoparticle suspension were placed onto a silicon wafer adhered to carbon tape, and the water was allowed to evaporate at 60 °C. The dry particles were sputter coated with a gold/palladium film using a Hummer 6.2 sputtering system (Anatech, Ltd.). Images were collected at 20 kV and 500,000X magnification.

The hydrodynamic diameter of the particles was analyzed using dynamic light scattering (DLS). DLS measurements were conducted using a Malvern Zetasizer Nano ZS equipped with a 633 nm red laser. Suspensions of approximately 100 ppm were prepared by adding 0.1 g nanoparticles to 10 mL of ultrapure water and sonicating for 1 h (20 min x 3). A 1 mL aliquot of the suspension was transferred to a ZEN0040 disposable cuvette and allowed to

equilibrate for 120 s before measurement. Measurement took place at 25 °C at a backscatter angle of 173°.

2.3 Textile Preparation, Modification, and Characterization

First, 0.3 g of cotton was cut into 1 cm x 1 cm squares and weighed. The fabric squares were washed by submersing in 50 mL of water in a conical tube and sonicating for 1 h, with the water being changed every 20 min. The fabric was dried at 100 °C for 1 h. A modification solution was prepared by adding 2.5 g citric acid ($\text{HOC}(\text{COOH})(\text{CH}_2\text{COOH})_2$), 1.5 g sodium phosphate dibasic (Na_2HPO_4), and 0.3125 g of α - or β -cyclodextrin to 25 mL of water. The cloth was added to the modification solution and stirred for 30 min. It was then dried at 110 °C for 10 min, and cured at 195 °C for 5 min. The modified cloth was rinsed with 60 °C water, dried at 110 °C, and weighed before further use.

Phenol red was used as an indicator to detect the presence of citric acid on modified cloth. Phenol red indicator was prepared by dissolving 0.1 g of phenolsulfonephthalein in 2.8 g of 0.01 M sodium hydroxide, NaOH, and adding 22.2 mL of water. Phenol red turns yellow in the presence of acids and fuchsia in the presence of bases. A square of unmodified and modified fabric were placed side-by-side on a weigh boat and a small, plastic transfer pipet was used to place a drop of indicator on each piece of fabric. The color of the fabric was observed as the solution was absorbed.

Infrared spectra of the nanoparticles and cloth were acquired using a Nicolet iS10 FTIR equipped with a diamond ATR, a HeNe laser source, and a KBr beam splitter. For each spectrum, 32 scans were acquired with a resolution of 4 cm^{-1} .

2.4 Adsorption of Zinc Oxide Nanoparticles to Textiles

2.4.1 Kinetics of Adsorption

A stock suspension was made by diluting 0.01 g of zinc oxide nanoparticles to a total mass of approximately 50 g with water and sonicating for 20 min, three times. Three samples and one control were prepared by transferring 10 g of stock suspension into 15 mL conical tubes. A square of fabric with known mass was added to each sample tube. The tubes were placed in the tube revolver for 2 h at 40 Hz. Aliquots of the suspension were taken at several intervals and diluted to 10 g with 5% HNO₃. The dilute solutions were analyzed for zinc concentration using inductively-coupled plasma optical emission spectroscopy (ICP-OES).

ICP-OES was conducted using a Perkin-Elmer Optima 4100DV system equipped with a GemTip cross-flow nebulizer, a AS90 autosampler (flow rate = 1.50 mL min⁻¹), an Echelle polychromator covering a UV range of 165-403 nm, and a 13 mm x 19 mm segmented-array charge-coupled-device detector (SCD). Argon was used as the carrier gas. Measurements were taken in the axial position, and three replicates were taken per measurement. A 60 s delay time was allowed before measurement, and a 45 s wash time was allowed between measurements. Standards in the concentration range of 0.5-8 ppm of Zn²⁺ were prepared using zinc nitrate hexahydrate (Zn(NO₃)₂ · 6 H₂O) in 5% HNO₃ to calibrate the instrument for each use.

2.4.2 Adsorption Isotherms

A 200 ppm stock suspension was made by diluting 0.01 g of zinc oxide nanoparticles to 50 g with water in a 50 mL conical tube; the suspension was sonicated for 1 h. Six dilute suspensions with known concentrations of approximately 200, 150, 100, 40, 20, and 10 ppm and a total mass of 10 g each were prepared in 15 mL conical tubes by diluting the stock suspension. A square piece of fabric with known mass was added to each of the suspensions.

The vials were continuously rotated on a tube revolver at 40 Hz for 3 h. After mixing, aliquots of the suspensions were diluted to 10 g with 5 % nitric acid (HNO_3). This sample was used to determine the quantity of free ZnO nanoparticles remaining in the suspension.

The cloths were carefully removed from the tubes using plastic thumb forceps with 12 x 12 serrated tips and patted dry with lab tissue to remove excess suspension. The dried cloths were then transferred to clean tubes and 10-20 g of 5 % HNO_3 was added to extract bound particles from the cloth. The cloths were removed after 5 min, and 10 mL of the resulting solution was filtered using a 0.2 μm syringe filter into to a 15 mL conical tube. The filtered solution was used to determine the quantity of bound ZnO nanoparticles that were adsorbed to the cloth. Both solutions were analyzed for zinc concentration using ICP-OES as described previously. Experiments were repeated at least twice for each cloth.

2.4.3 Scanning Electron Microscopy

Scanning electron microscopy-energy dispersive x-ray spectroscopy (SEM-EDX) was used to confirm nanoparticle adsorption to cloth and determine its elemental composition. One image of unmodified mercerized/bleached cloth with EDX mapping was acquired with the S4800 while modified, mercerized/bleached cloth images and spectra were acquired using a SU6600 instrument under the direction of Mr. George Wetzal at Clemson University Advanced Materials Research Lab. Cloths were prepared in a manner similar to the nanoparticles using the highest concentration from the adsorption experiment. First, cloths were placed on carbon tape and grounded with PELCO colloidal graphite with an isopropanol base (Ted Pella, Inc.), then they were sputter-coated coat with a gold/palladium film. Images were collected at 20 kV and 200X magnification

2.4.4 Wash Durability

A stock suspension was prepared by diluting 0.011 g of ZnO nanoparticles to 55 g with water in a 50 mL conical tube. Five sample suspensions were prepared by transferring 10 g of stock suspension into 15 mL conical tubes and a square of unmodified, mercerized cloth with known mass was added to each sample tube. Sample suspensions were placed on the tube revolver for 3 h at 40 Hz, then, the tubes were taken off the revolver. The cloths were removed from the tubes with plastic forceps, patted dry with lab tissue, transferred to a watch glass, and heat dried at 60 °C for 5 min. The cloths were washed by submersion in water for approximately 3 s and then dried by patting with lab tissue and heating in an oven at 60 °C for 5 min. Each cloth was washed by dipping in water 0, 2, 4, 6, or 8 times, and pat dry between washes. Each washed cloth was transferred to a 50 mL conical tube and 20 g of 5% HNO₃ was added. Cloth solutions were shaken for 5 min, filtered using a 0.2 μm syringe filter, and analyzed for Zn concentration using ICP-OES, as described in Section 2.4.1.

CHAPTER 3: RESULTS AND DISCUSSION

3.1 Nanoparticle Characterization

3.1.1 Crystal Size

The X-Ray powder diffraction spectrum of the ZnO nanoparticles is shown in Figure 6. Peaks observed at 2θ values of 32, 34, 36, 48, 57, 63, 68° match the literature reported values for zinc oxide nanoparticles.⁹ The XRD peaks indicate the formation of the pure phase, wurtzite structure of ZnO.⁹

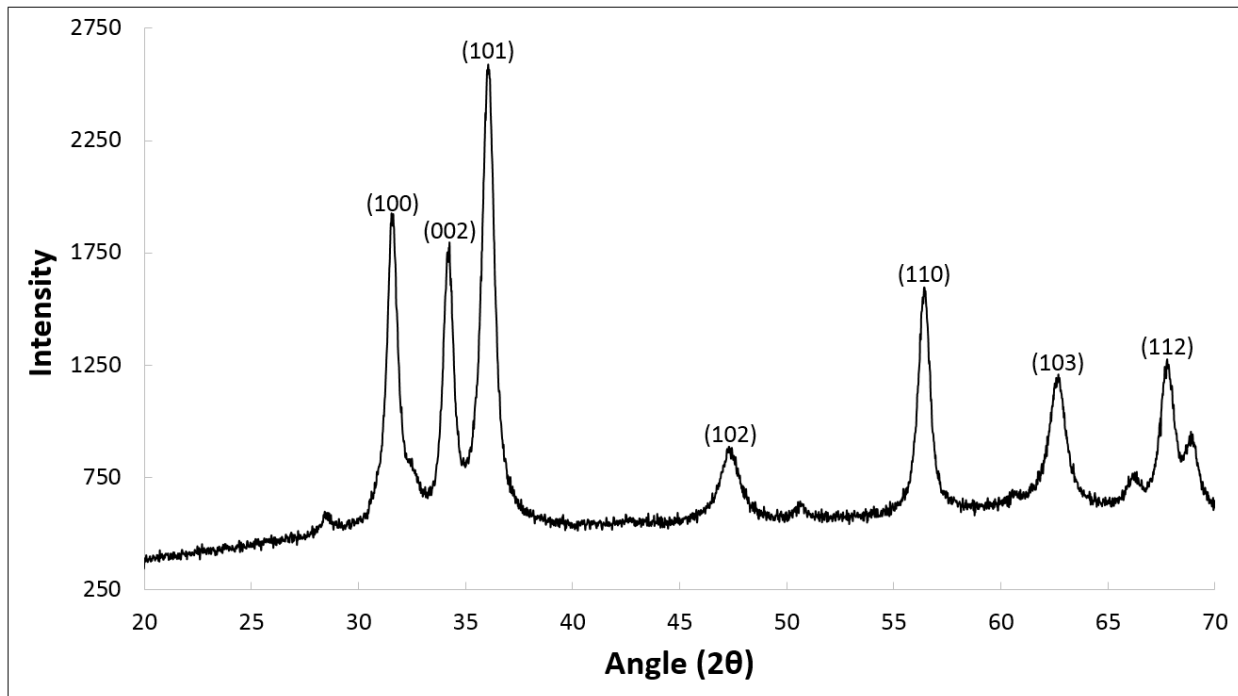


Figure 6. X-ray powder diffraction spectrum of zinc oxide nanoparticles.

The Scherrer equation can be used to approximate the crystal size (τ):

$$\tau = \frac{K\lambda}{\beta \cos \theta} \quad (5)$$

where K is the shape factor ($K = 0.9$), λ is the X-ray wavelength in nm ($\lambda = 0.178899$ nm),

β is the width at half maximum intensity in radians for each peak, and θ is the Bragg angle in radians for each peak. Table 1 shows the parameters used in the Scherrer equation and the calculated crystal sizes. The average crystal size was estimated to be approximately 13 ± 2 nm, which matches previously reported values.²² The approximate crystallinity was estimated to be $80 \pm 9\%$ by comparing the area of the crystalline peaks to the total area including the background, which is not flat for amorphous components.

Table 1. Parameters used in the Scherrer equation and the crystal size of powder zinc oxide nanoparticles.

Lattice Plane	θ ($^\circ$)	β ($^\circ$)	τ (nm)
(100)	31.633	0.85	11
(002)	34.236	0.75	13
(101)	36.086	0.87	11
(110)	56.42	0.70	15
(112)	67.80	0.71	16
Average			13 ± 2

Figure 7 shows an SEM image of the zinc oxide nanoparticles. Individual nanoparticles appear to be less than 10 nm, but the low image resolution makes it difficult to measure the size quantitatively. Also, it should be noted that the image may show the gold and palladium coating rather than the nanoparticles themselves.

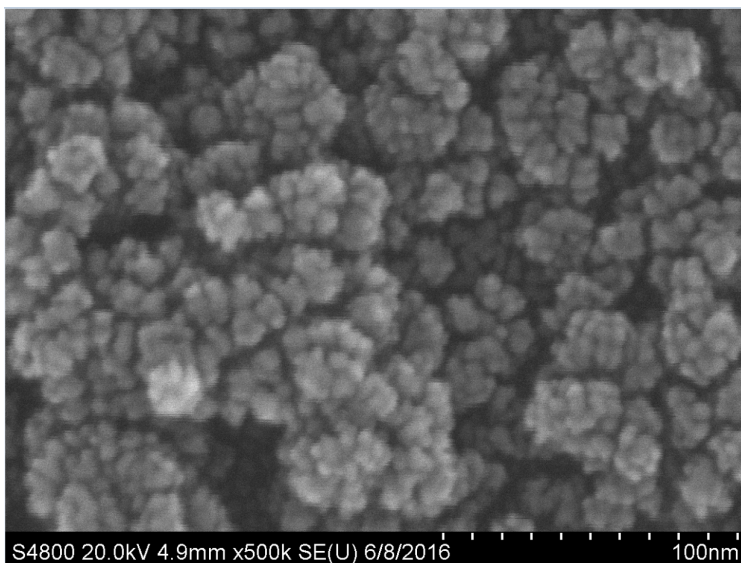


Figure 7. SEM image of zinc oxide nanoparticles.

3.1.2 Hydrodynamic Diameter

The hydrodynamic diameter represents the size of the nanoparticle aggregates in water. Figure 8 shows the size distribution of the nanoparticles measured using dynamic light scattering (DLS). Three measurements of a single sample were taken subsequently, with approximately 2 min between runs. The second had a slightly higher average diameter than the first one, but the third run had a much smaller increase. Values of average hydrodynamic diameter and polydispersity index for each run is shown in Table 2. The average hydrodynamic diameter was found to be 75 ± 2 nm. The average particle diameter of Run 2 was approximately 3 nm larger than Run 1, while Run 3 was approximately 1 nm larger than Run 2. This indicates that the particles aggregate, but do not sediment, meaning the suspension was stable over a short time scale. Longer time scales were not tested, although at higher concentrations, sedimentation was visible. The polydispersity index (PDI) is a measure of the variation of aggregate sizes. A low PDI correlates to a small variation, while a high PDI corresponds to a greater amount of size variation. Generally, a PDI of 0.5 or higher is considered to be polydisperse. The zinc oxide nanoparticles had an average PDI of 0.191 ± 0.005 , indicating

they were monodisperse.

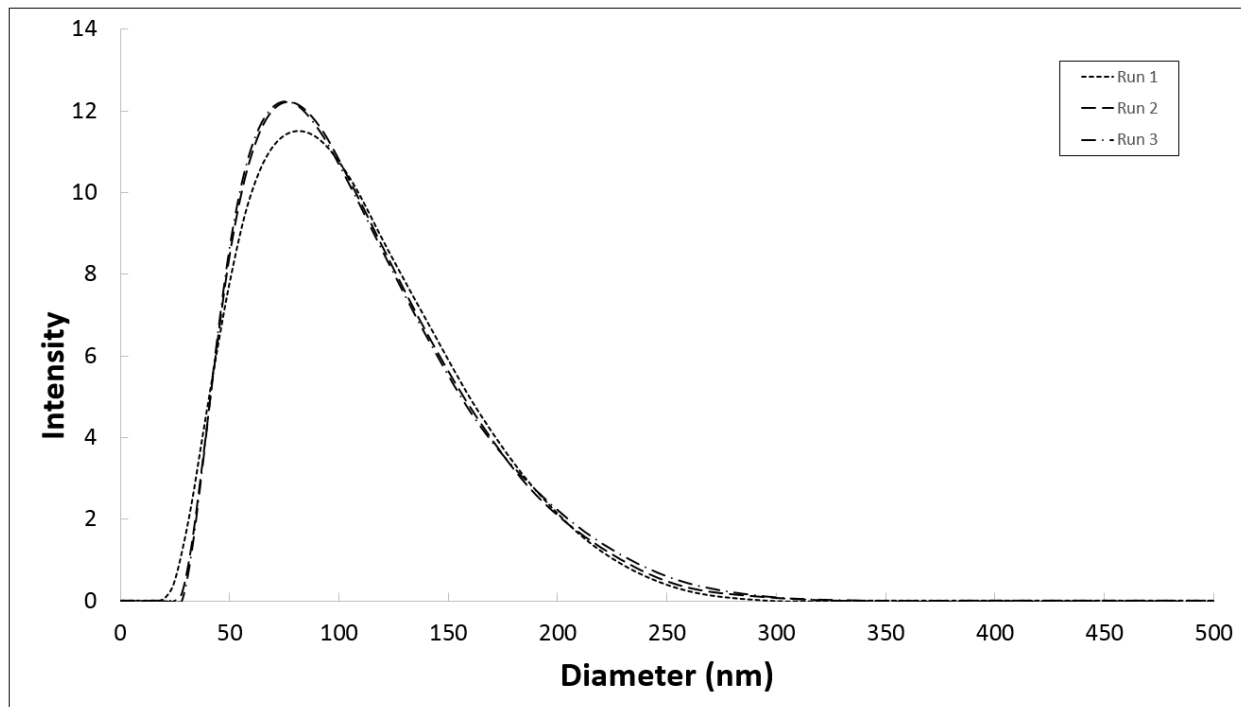


Figure 8. Hydrodynamic diameter distribution of zinc oxide nanoparticles.

Table 2. Hydrodynamic diameters and polydispersity indices of zinc oxide nanoparticles suspended in water.

Run	Diameter (nm)	PDI
1	72.29	0.172
2	75.16	0.165
3	76.21	0.175
Average	75 ± 2	0.171 ± 0.005

3.2 Fabric Modification

Fabrics were modified with α - or β -cyclodextrin using citric acid as a cross-linker, as shown in Figure 5. Phenol red was used to determine the presence of citric acid on the modified cloth. The indicator turns from red in a neutral environment to yellow in the presence of

acid. This color change is shown in Figure 9 and was the same for all cloths. The squares in the upper left are unmodified cloth, which turns red. The squares in the upper right are cloth modified with α -cyclodextrin (α -CD), and the squares in the bottom are cloth modified with β -cyclodextrin (β -CD), both of which turn yellow indicating the presence of citric acid on the cloth.

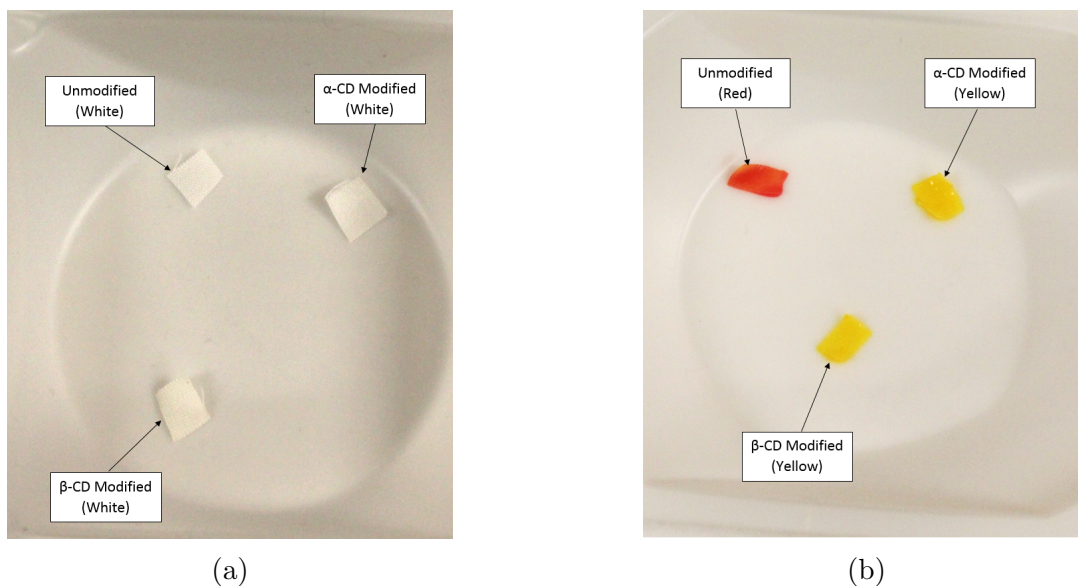


Figure 9. Change in color of mercerized cotton cloth (a) before and (b) after addition of phenol red.

FTIR spectra of α -CD and β -CD modified mercerized/bleached cloth were acquired to confirm modification and are shown in Figures 10 and 11, respectively. A prominent peak at 1650 cm^{-1} in the citric acid spectrum corresponds to the carbonyl stretching mode. This peak is present in the spectrum of the modified cotton at 1700 cm^{-1} but is not present in the unmodified cotton spectrum, and confirms the presence of citric acid on the modified cotton. The shift in peak position is caused by the conversion of the carboxylic acids in the citric acid to ester groups.²³ The peak at 1700 cm^{-1} is much more evident in the β -CD modified cloth (Figure 11) than in the α -CD modified cloth (Figure 10), for an unknown reason. There is a very small peak around 2900 cm^{-1} in the spectrum of the β -CD modified

cloth (Figure 11) that is only slightly resolved from the normal alkane stretching peak of the cotton. However, it lines up with the analogous peak in the β -CD spectrum, and so may be evidence of the presence of β -CD on the modified fabric.

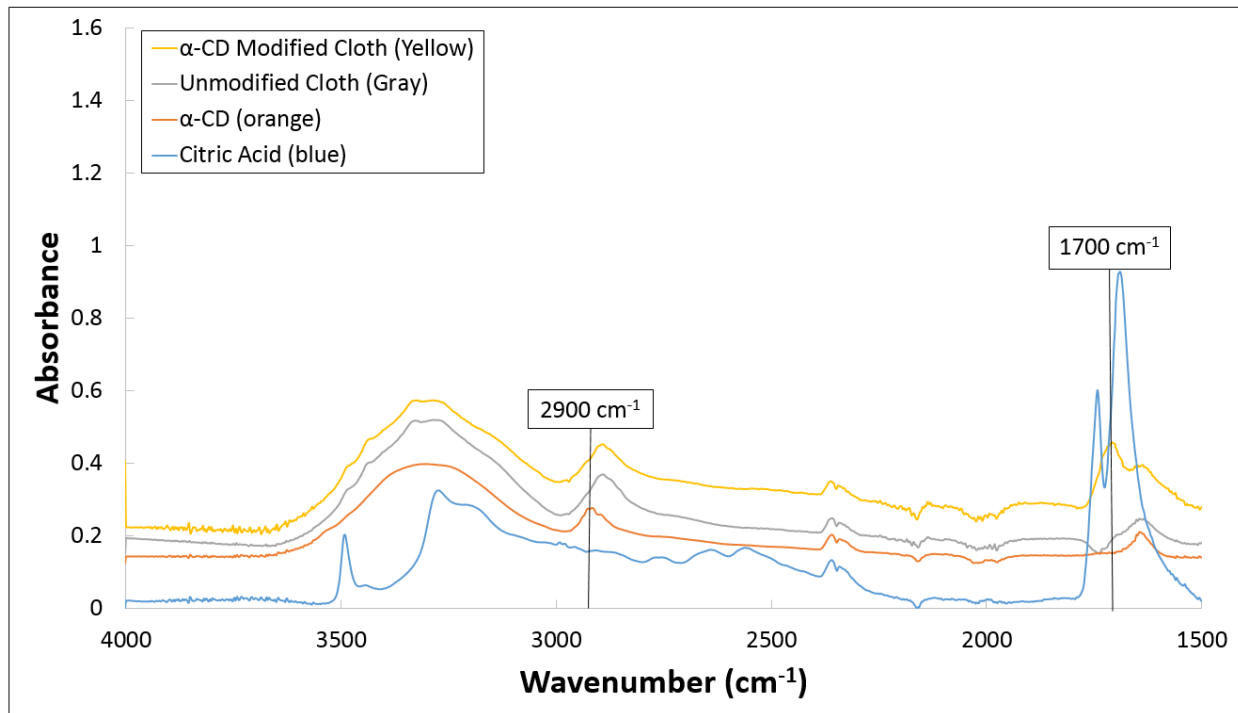


Figure 10. Infrared spectrum of citric acid, α -CD, unmodified mercerized/bleached cloth, and α -CD modified mercerized/bleached cloth.

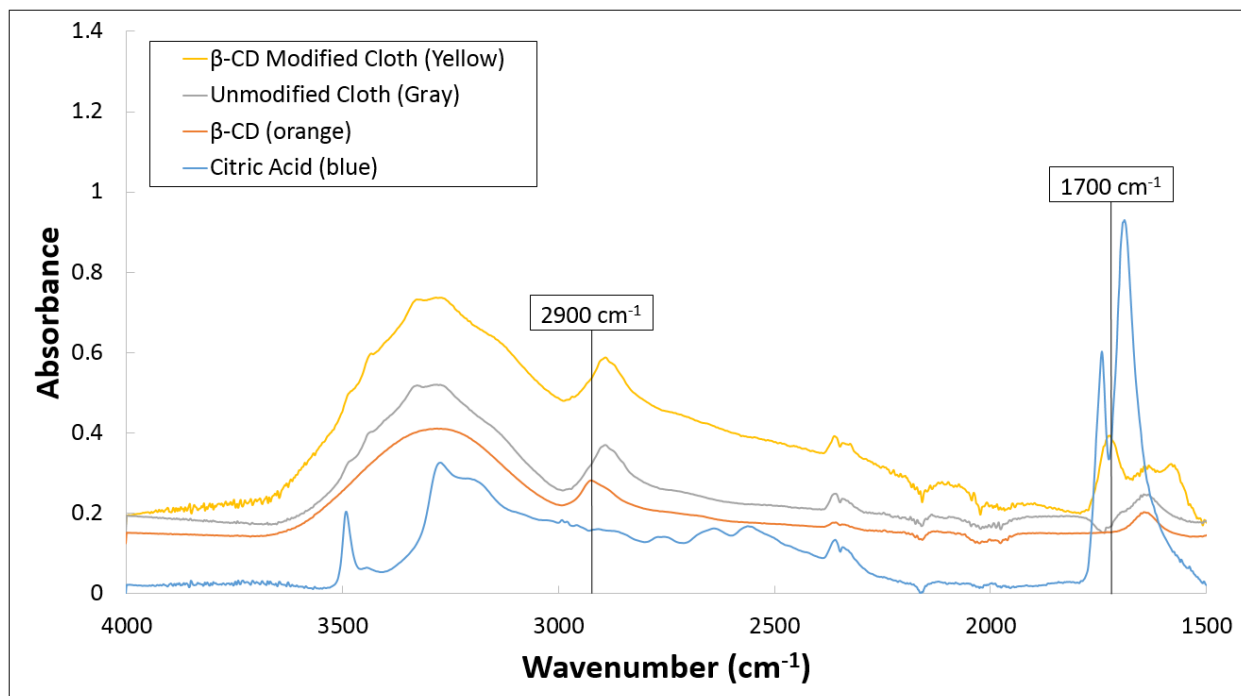


Figure 11. Infrared spectrum of citric acid, β -CD, unmodified mercerized/bleached cloth, and β -CD modified mercerized/bleached cloth.

Figure 12 shows the percentage increase in the mass of cloths after modification. First, cloths were modified by adding the citric acid linker in the absence of α - or β -CD. The mass of the cloth increased by an average of $7.4 \pm 0.3\%$. Then, cloths were modified with the citric acid linker in the presence of the α - or β -CD, and the average mass increase was $21.1 \pm 0.3\%$. Since this increase is larger than the increase without the α - or β -CD, it confirms the addition of the CD. Table 3 shows the percent mass (w/w) of components in modified cloth. The modified cloth contains approximately 6.9% w/w citric acid and 10.5% w/w CD. Table 4 shows the amount of cloth covered with citric acid, α -CD, and β -CD in moles per square centimeter. Areas of cloth were not directly measured but were estimated to be approximately 1 cm². The average mass of the squares of cloth used in adsorption experiments were assumed to be the mass of one square centimeter of cloth (0.004 g for unbleached, 0.005 g for bleached, and 0.007 g for mercerized/bleached). Bleached cloth adsorbed more citric acid

and cyclodextrin than unbleached cloth, and mercerized/bleached cloth adsorbed the most citric acid and cyclodextrin. Table 4 shows that not every citric acid molecule is bound to a cyclodextrin molecule, indicating some free citric acid is available for binding on the cloth surface.

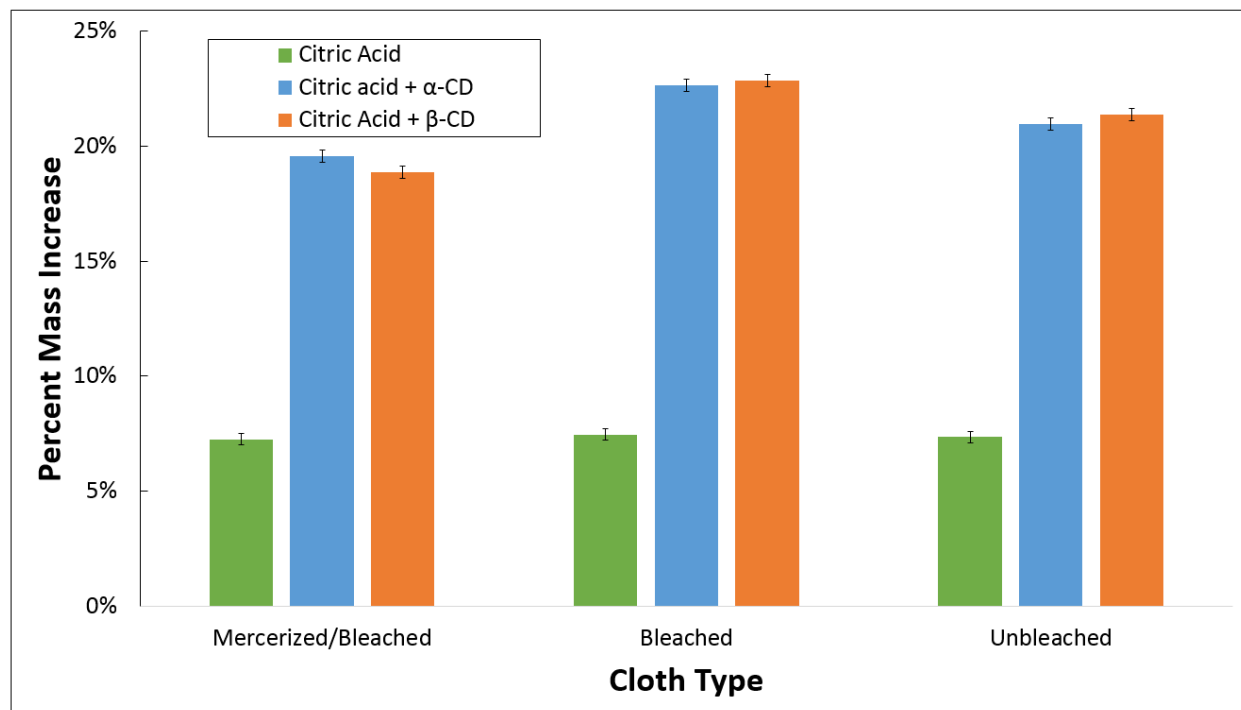


Figure 12. Percentage increase in cloth mass after modification with citric acid alone (green), and citric acid with α -CD (blue) or β -CD (orange).

Table 3. Percent mass of components on modified cloth. The uncertainties in percentages are between 0.2 and 0.3% as determined by error propagation.

Component	Mercerized/Bleached	Bleached	Unbleached
Citric Acid	6.8%	7.0%	6.9%
Citric Acid + α -CD	9.6%	11.5%	10.5%
Citric Acid + β -CD	9.1%	11.7%	10.8%

Table 4. Approximate moles of citric acid, α -CD, and β -CD per square centimeter of cloth.

Cloth Type	Citric acid	α-CD	β-CD
Mercerized/Bleached	2.6×10^{-6}	7.9×10^{-7}	6.5×10^{-7}
Bleached	2.0×10^{-6}	7.3×10^{-7}	6.4×10^{-7}
Unbleached	1.7×10^{-6}	5.8×10^{-7}	5.0×10^{-7}

3.3 Adsorption

3.3.1 Adsorption Kinetics

Different types of cloth were added to zinc oxide nanoparticle suspensions and the zinc concentration was monitored over time to determine the time required for the system to reach equilibrium. Figure 13 shows the nanoparticle concentration over time for these cloths. As is expected, the concentration decreases rapidly at first as adsorption occurs, and then reaches a relatively constant value as the system reaches equilibrium. With the exception of the outlying second data point of the control, which contained no fabric, there is only a slight decrease in concentration which can be attributed to some adsorption of the nanoparticles to the plastic container. Table 5 states the decreases in the concentration over the entirety of the experiment and the decreases over the last hour of the 2 h experiment. The decrease during the second hour is much lower than the entirety of the experiment. The concentration decreased by less than 15% during the second hour in most cases. This indicates that two hours is enough time for the zinc oxide nanoparticles and the cotton cloth to reach equilibrium. All further adsorption experiments were allowed to equilibrate for at least 3 h to ensure complete equilibration.

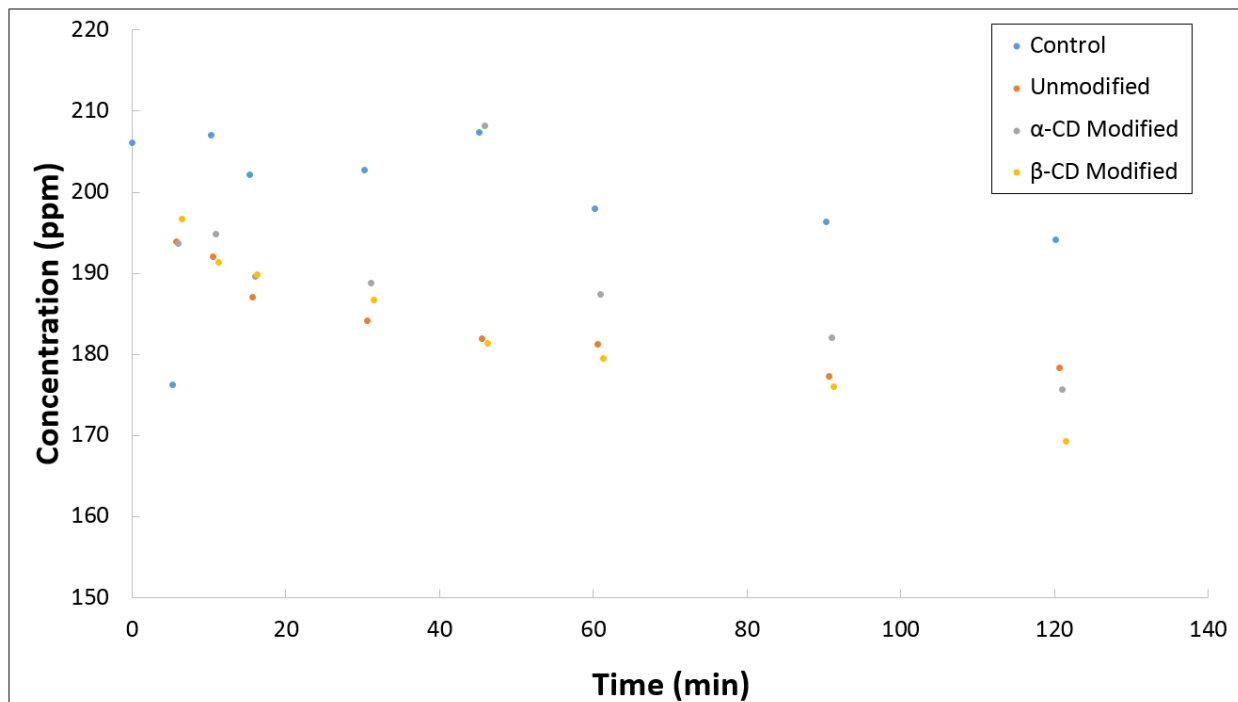


Figure 13. ZnO concentration over time in the presence of cotton cloth samples.

Table 5. Decrease in nanoparticle concentration over time.

Sample	Overall (ppm)	Second Hour (ppm)	% Decrease
Control	51.52	3.780	7.337 %
Unmodified	67.32	2.949	4.381 %
α -CD	69.99	11.73	16.75 %
β -CD	76.39	10.22	13.38 %

3.3.2 Adsorption Isotherms

Zinc oxide concentrations in the equilibrium solution and on the cloth were used to create adsorption isotherms for each type of fabric with each modification. Figures 15-17 show the adsorption isotherms of the nanoparticles to mercerized/bleached cloth, bleached cloth, and unbleached cloth, respectively. Adsorption data for the nanoparticles onto unmodified cloth is shown in blue. Data for cloth modified with α -CD is shown in orange, and data for cloth

modified with β -CD is shown in green. These data were fit with the Langmuir equation (Equation 2), shown as dotted lines on the graph. Fitting parameters yield the adsorption capacity, Q_0 , and b , which is related to the binding energy. Higher values of b may indicate stronger binding if differences in entropy of adsorption are negligible. Values for Q_0 and b are summarized in Table 6. Uncertainties are standard deviations from the fit as determined by the Vernier LoggerPro fitting software.²⁴ Uncertainties, including the RMSE, are higher for modified cloth than unmodified cloth samples, which may be due to variation in distribution of cyclodextrin from sample to sample.

Adsorption isotherms of the unmodified cloths are shown in Figure 14. Bleached causes a decrease in capacity from 22 mg ZnO/g cloth to 17 mg ZnO/g cloth, although the uncertainty suggests that these values are almost indistinguishable. Since the mercerized cloth is also bleached, a similar decrease in capacity is expected, but instead the capacity is slightly higher than the bleached cloth at 20 mg ZnO/g cloth, suggesting the increased surface area from the mercerization process does in fact increase capacity. For unmodified cloths, bleached cloth has the highest binding strength, followed by unbleached cloth, and mercerized cloth has the lowest binding strength. The bleached cloth likely has a higher strength due to the increased polarity of the carbonyls over the hydroxyls of unbleached cloth. Mercerized cloth can be less reactive due to its form,¹⁵ which might be why it has the lowest binding strength.

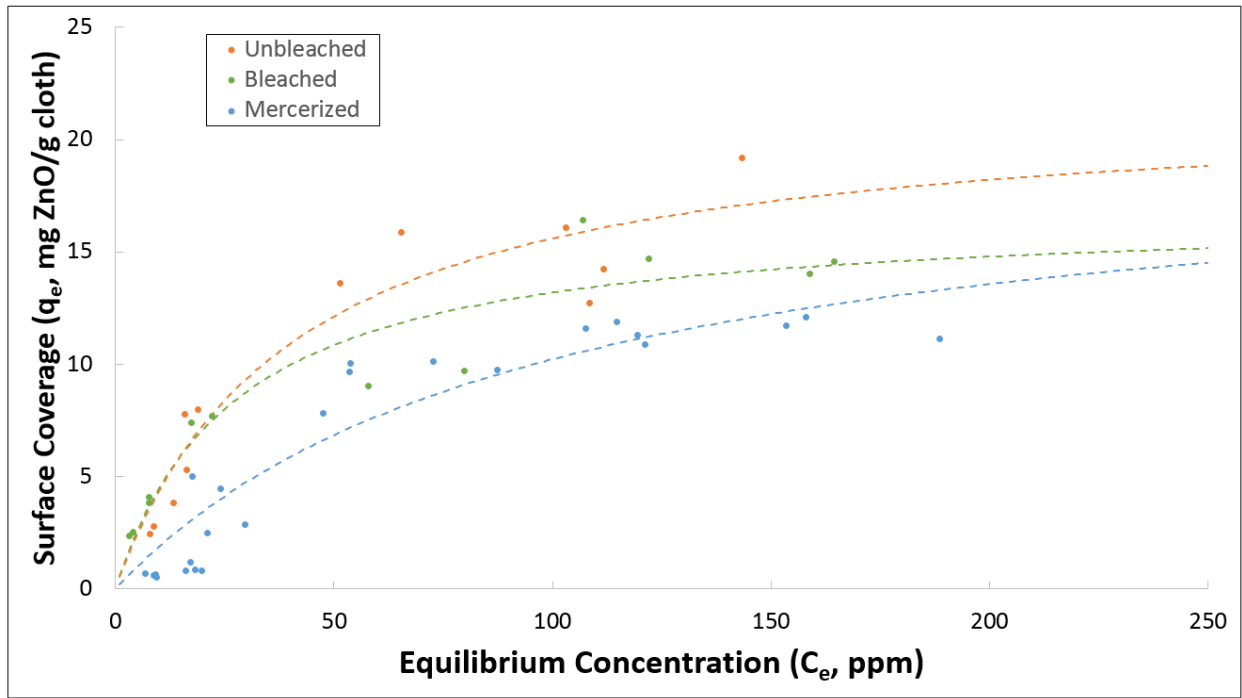


Figure 14. Adsorption isotherm for unmodified cloths.

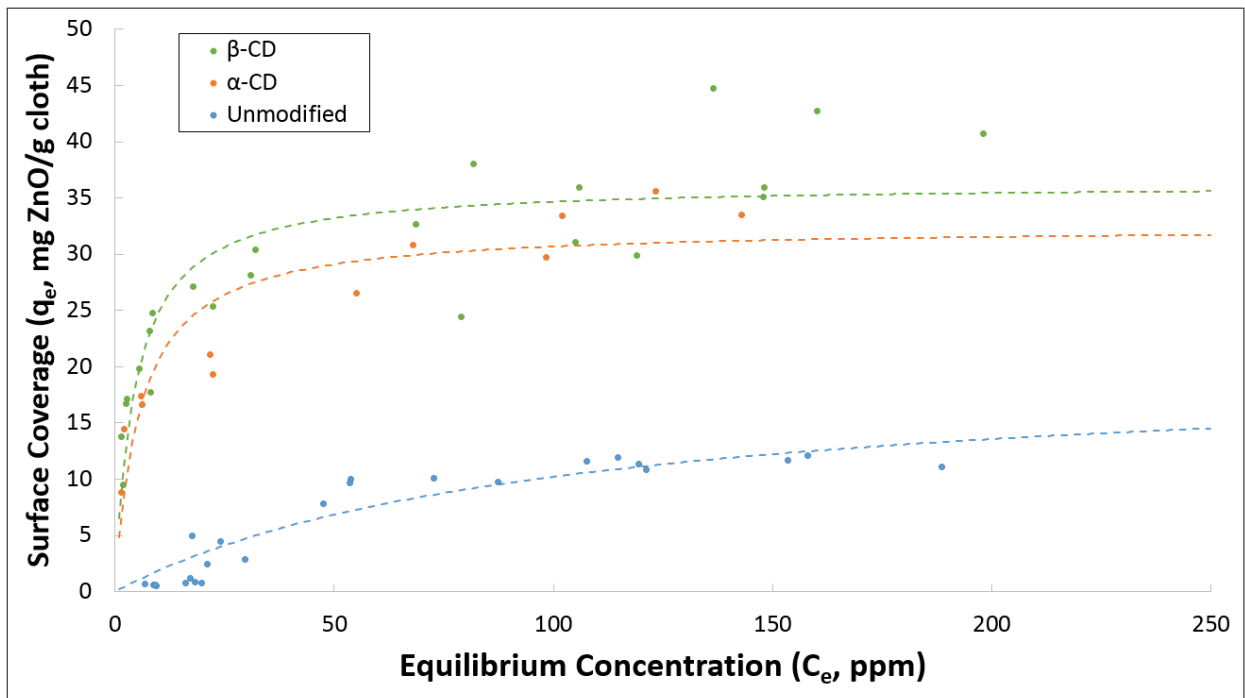


Figure 15. Adsorption isotherms for mercerized cloth.

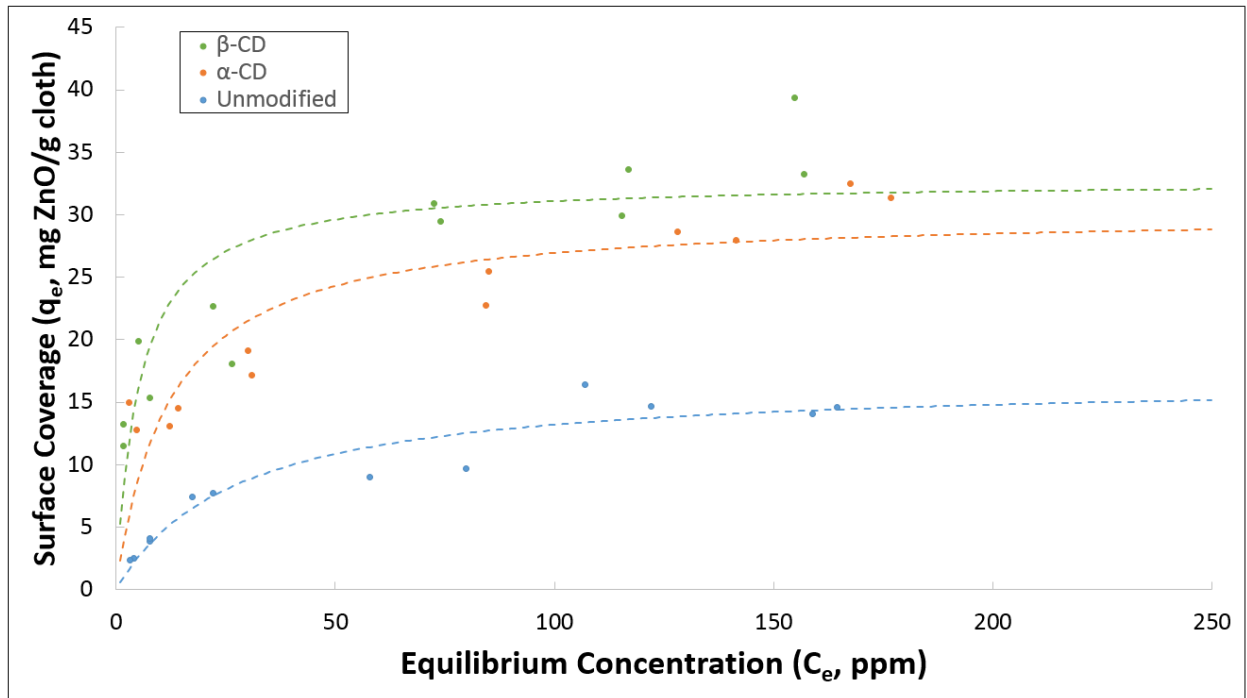


Figure 16. Adsorption isotherm for bleached cloth.

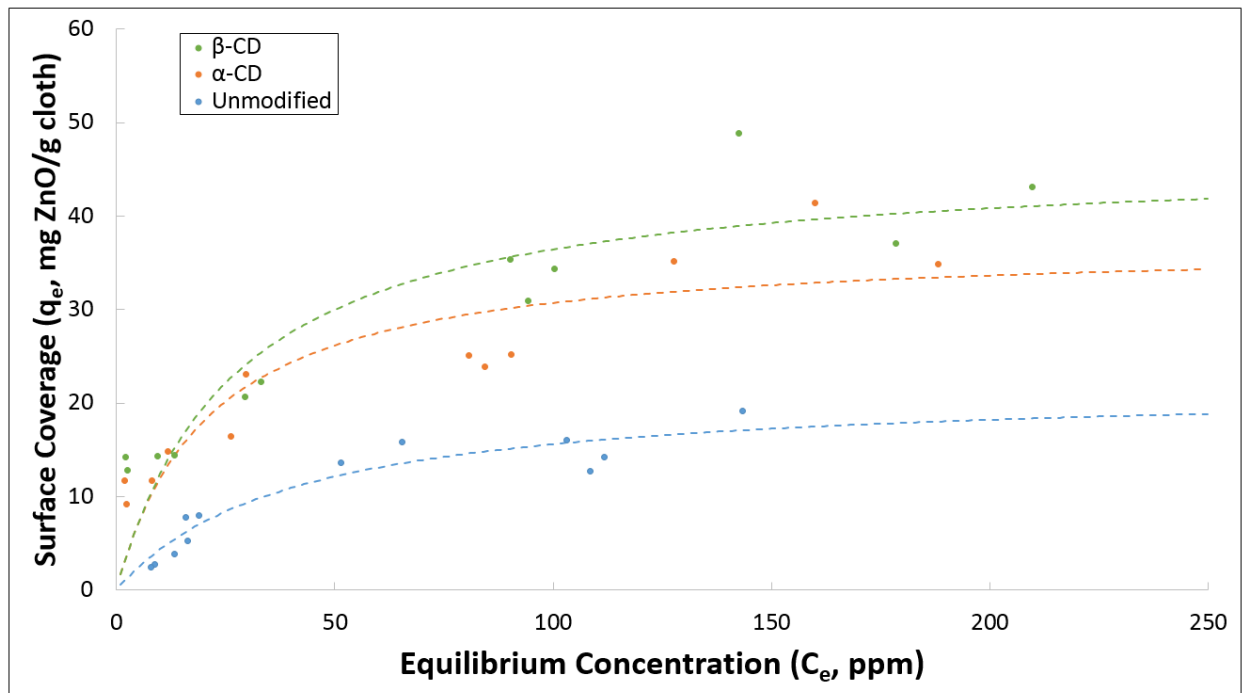


Figure 17. Adsorption isotherm for unbleached cloth.

In all cases, cloth modified with α -CD or β -CD had greater adsorption capacities and binding strengths than unmodified cloth. This is likely due to the increase in the number of available hydroxyl groups on the fiber from the presence of the CD. Percent increase in adsorption capacity after modification ranged from 61-80% in α -CD modified cloth, and 80-112% in β -CD modified cloth. Likewise, the percent increase in relative binding strength after modification ranged from 90-1601% for α -CD modified cloth and from 46-2027% for β -CD modified cloth. This indicates that modification successfully increased adsorptivity in all cases. The β -CD modified fabrics had higher adsorption capacities and relative binding strengths than the α -CD modified fabrics. This increased adsorptivity is possibly the result of the additional glucopyranose unit in β -CD, which provides 3 additional hydroxyl groups per CD molecule for binding to nanoparticles.

However, when the cloths were modified with α - or β -CD, mercerized/bleached cloth yielded the highest relative binding strength. This is inconsistent with what was observed for unmodified cloth, in which binding to mercerized/bleached cloth was the weakest. Unbleached cloth had the lowest strength among the three α - or β -CD modified cloths. For all modifications, unbleached cloth has a higher adsorption capacity than mercerized cloth, which has a higher capacity than bleached cloth.

Table 6. Adsorption capacities (Q_o in mg ZnO/g cloth), relative binding strengths (b in ppm⁻¹) and root mean square error (RMSE) from the fit to the Langmuir equation for each type of cloth that was tested.

Cloth Type	Q_o	% Inc Q_o	b	% Inc b	RMSE
Mercerized/Bleached					
Unmodified	20 ± 3		0.010 ± 0.003		1.634
α -CD	32 ± 9	61%	0.17 ± 0.05	1601%	3.755
β -CD	36 ± 8	80%	0.22 ± 0.05	2027%	4.68
Bleached					
Unmodified	17 ± 4		0.22 ± 0.05		1.593
α -CD	30 ± 10	80%	0.08 ± 0.03	126%	4.257
β -CD	33 ± 12	94%	0.19 ± 0.08	427%	4.942
Unbleached					
Unmodified	22 ± 4		0.025 ± 0.008		1.877
α -CD	37 ± 14	70%	0.05 ± 0.02	90%	5.436
β -CD	46 ± 15	112%	0.04 ± 0.01	46%	6.027

3.3.3 Energy Dispersive X-Ray Spectra of Cloth with Nanoparticles

Unmodified and modified mercerized/bleached cloths were prepared with adsorbed nanoparticles such that the surface coverage was near the adsorption capacity. These cloths were analyzed with SEM-EDX. Figure 18 shows a high magnification image of fairly uniform clusters of nanoparticles adsorbed onto the cloth, though again these may be the gold and palladium coating. Figure 19 shows an EDX map of carbon, oxygen, and zinc on the cloth, clearly showing that zinc oxide is present, but the distribution is not uniform. Figure 20 shows three SEM images used for EDX spectroscopy of nanoparticles on (a) unmodified, (b) α -CD modified, and (c) β -CD modified mercerized/bleached cloth. The corresponding EDX spectra are shown in Figure 21. The weight percentages of zinc and other elements is listed in Table 7. The phosphorus seen in the modified cloths comes from the Na_2HPO_4 used as a catalyst in the modification process. EDX spectra indicate that modified cloth has more zinc oxide nanoparticles adsorbed to it than unmodified cloth, and that β -CD modified cloth has more zinc oxide adsorbed than the α -CD modified cloth. However, these

values were obtained by the microscope at the surface level, and do not account for nanoparticles trapped within the cloth fibers. Additionally, the area sampled by the SEM was approximately 0.003 cm^2 , whereas the cloths sampled by the ICP-OES in determining surface coverage, were approximately 1 cm^2 . Since the nanoparticles are dispersed irregularly, these images may not be accurate representations of the entirety of the cloth. As such the zinc abundance measured by EDX cannot be directly compared to the adsorption capacities determined using ICP-OES. However, the trend seen in these data seems to support the adsorption isotherm evidence that the modification enhances adsorptivity of nanoparticles and that β -CD increases enhancement more than α -CD.

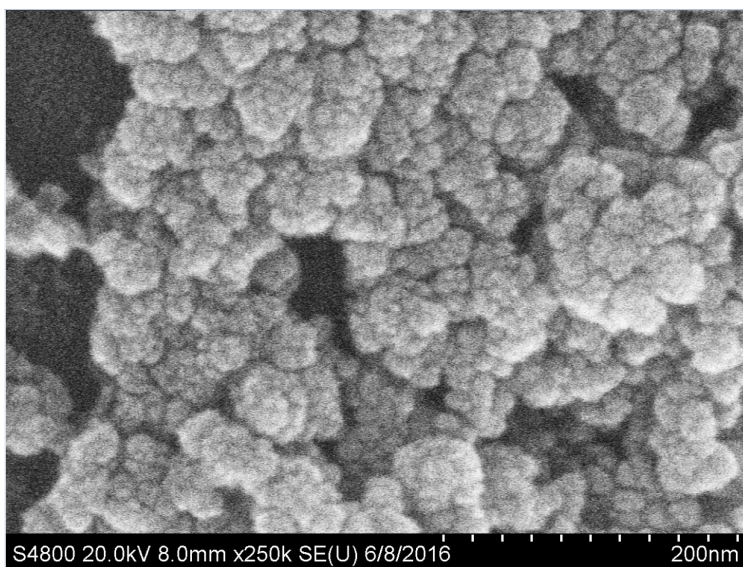
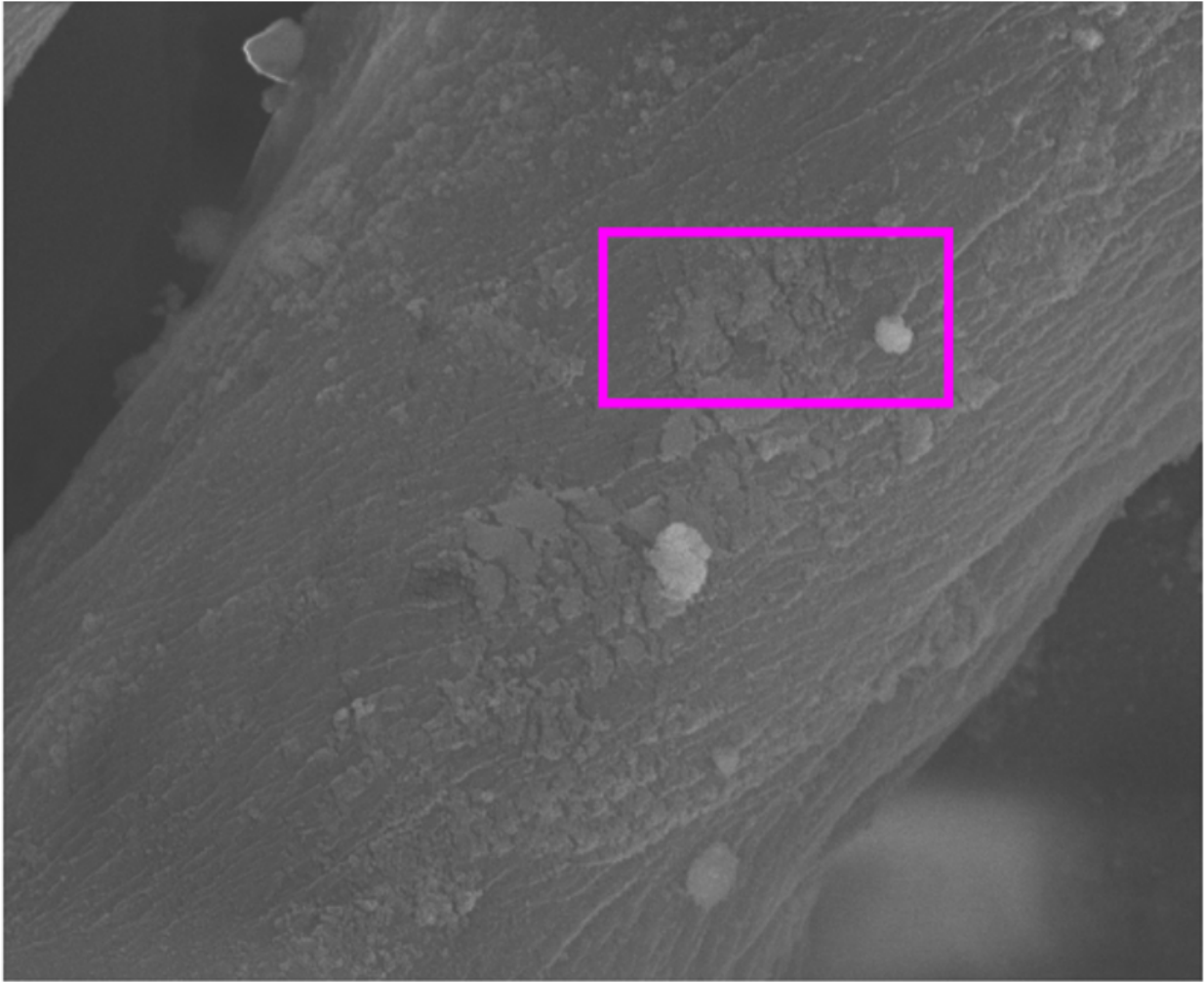
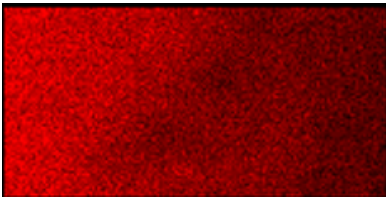


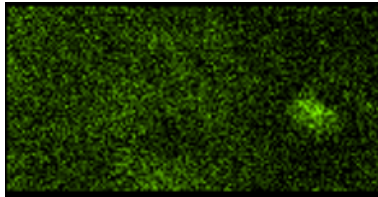
Figure 18. SEM image of zinc oxide nanoparticles bound onto unmodified cloth.



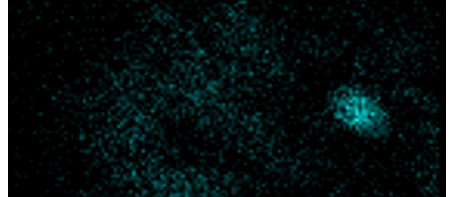
(a)



(b)



(c)



(d)

Figure 19. EDX map of cotton fiber highlighting (b) carbon (red), (c) oxygen (green), and (d) zinc (blue).

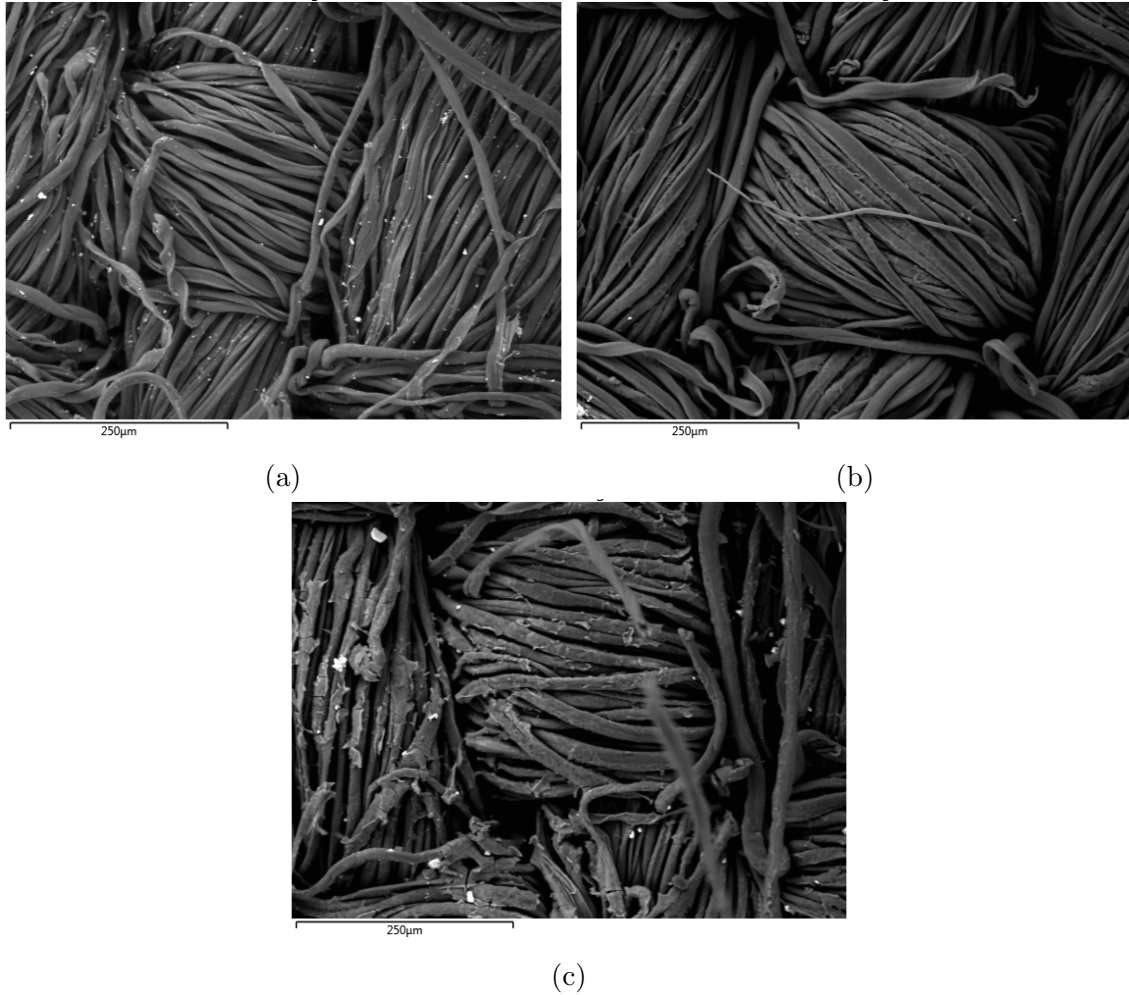


Figure 20. SEM image of (a) unmodified, (b) α -CD modified, and (c) β -CD modified mercerized/bleached cloth. White specks are clusters of zinc oxide nanoparticles.

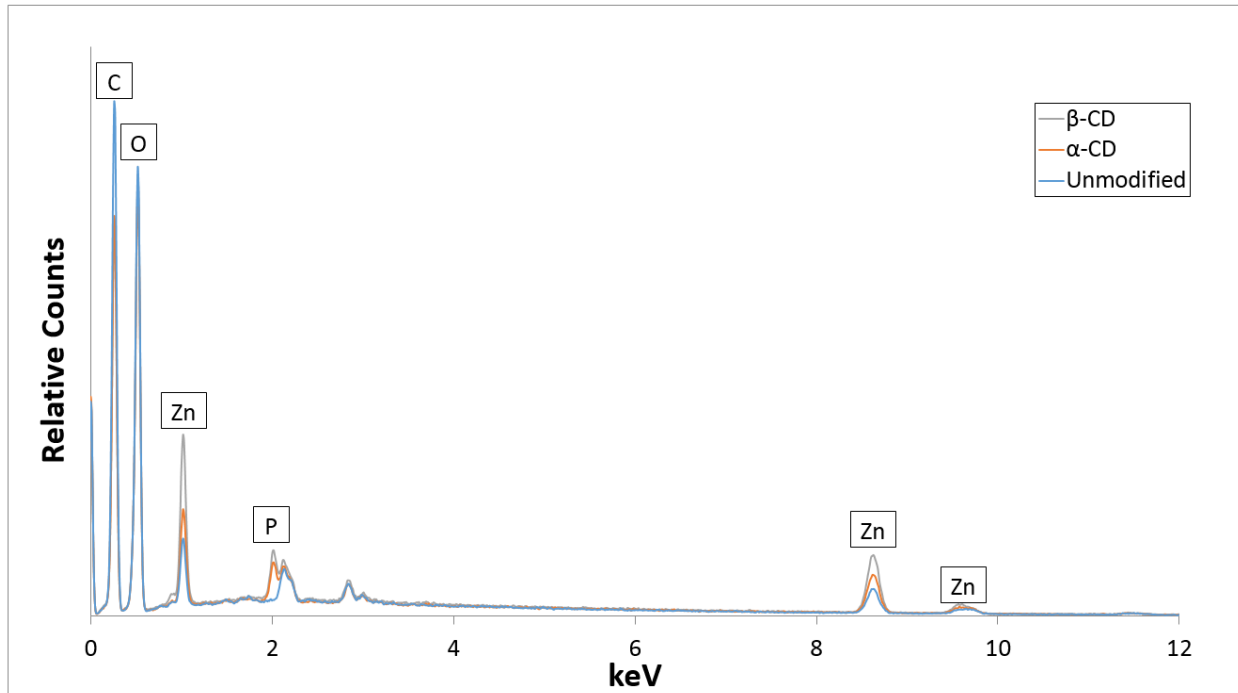


Figure 21. Elemental analysis of unmodified (blue), α -CD modified (orange), and β -CD modified (gray) cloth.

Table 7. Elemental weight percentages for each type of cloth. Uncertainties are between 0.2 and 0.3 %.

Cloth Type	Carbon	Oxygen	Zinc	Phosphorus
Unmodified	47.4 %	44.1 %	8.5 %	0.0 %
α -CD Modified	44.8 %	41.0 %	13.4 %	0.8 %
β -CD Modified	43.3 %	37.6 %	18.1 %	1.0 %

3.4 Wash Durability

Fabrics were tested for wash fastness with adsorbed nanoparticles. However there was not much change in the surface coverage with the washing method for either type of cloth. Modification did seem to affect wash durability, but the test is inconclusive. A different washing procedure that is similar to a traditional washing machine cycle using detergent may show a decrease in coverage.

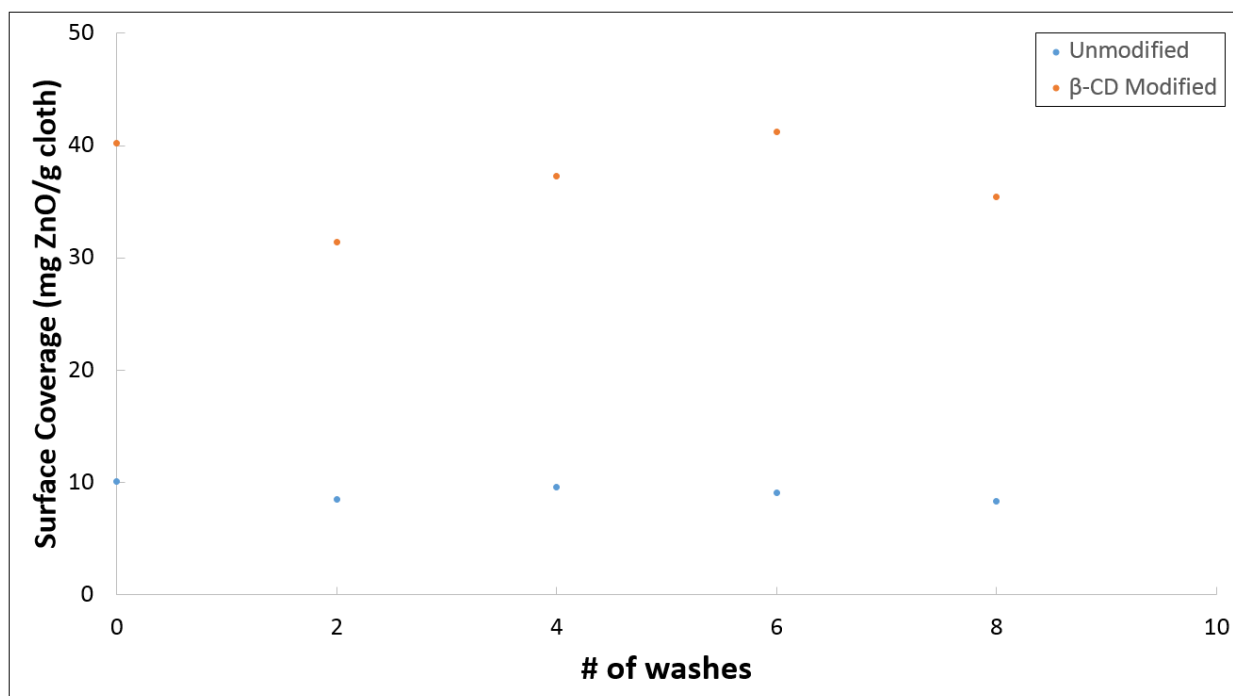


Figure 22. Chart of the change in coverage with consecutive washes.

CHAPTER 4: CONCLUSION

It was predicted that bleaching the cloth would increase binding strength due to the increased polarity of carbonyls compared to hydroxyls, and it was shown that binding strength for bleached cloth was higher in all cases, but adsorption capacity was lower. It was thought that mercerization would increase adsorption capacity and binding strength over unmercerized cloth. The mercerized/bleached cloth did have a higher adsorption capacity than bleached cloth, but it was lower than unbleached cloth. Also, unmodified mercerized/bleached cloth had a lower binding strength than the other cloths, but modified mercerized/bleached cloth had higher strength than other modified cloths.

It was hypothesized that modification of the cloths would increase adsorption capacity and binding strength, and it did in all cases. Modification with β -cyclodextrin increased these values more than modification with α -cyclodextrin in all cases, except for the binding strength of unbleached cloth. As a result, mercerized and bleached cloth modified with β -cyclodextrin would be the best candidate for use in antimicrobial textiles.

REFERENCES

- [1] Hensley, B. J.; Monson, J. R. Hospital-acquired infections. *Surgery (Oxford)* **2015**, *33*, 528–533.
- [2] Hidron, A. I.; Edwards, J. R.; Patel, J.; Horan, T. C.; Sievert, D. M.; Pollock, D. A.; Fridkin, S. K. Antimicrobial-resistant pathogens associated with healthcare-associated infections: Annual summary of data reported to the National Healthcare Safety Network at the Centers for Disease Control and Prevention, 2006-2007. *Infect. Control and Hosp. Epidemiol.* **2008**, *29*, 996–1011.
- [3] Fijan, S.; Turk, S. Š. Hospital textiles, are they a possible vehicle for healthcare-associated infections? *Int. J. Environ. Res. Public Health* **2012**, *9*, 3330–3343.
- [4] Neely, A. N.; Maley, M. P. Survival of *Enterococci* and *Staphylococci* on hospital fabrics and plastics. *J. Clin. Microbiol.* **2000**, *38*, 724–726.
- [5] Gorjanc, M.; Jazbec, K.; Šala, M.; Zaplotnik, R.; Vesel, A.; Mozetič, M. Creating cellulose fibres with excellent UV protective properties using moist CF₄ plasma and ZnO nanoparticles. *Cellulose* **2014**, *21*, 3007–3021.
- [6] Saleh, R.; Djaja, N. F. Transition-metal-doped ZnO nanoparticles: Synthesis, characterization and photocatalytic activity under UV light. *Spectrochim. Acta. Part A* **2014**, *130*, 581–90.
- [7] Maiti, K. A.; Maiti, A.; Neogi, R.; Kothari, D. C. Differential susceptibility of gram positive and gram negative bacteria towards ZnO nanoparticles. *Int. J. Chem. Phys. Sci.* **2014**, *3*, 68–77.
- [8] Ambika, S.; Sundrarajan, M. Synthesis of β -cyclodextrin/ZnO nanocomposites and its

- improved antibacterial activity on cotton fabric. *World J. Pharm. Pharm. Sci.* **2014**, *3*, 751–761.
- [9] Darsanasiri, N. D. *Synthesis and property investigation of metal-based nanomaterials for biotechnological applications*; Western Carolina University: Cullowhee, NC, 2014.
- [10] Hiemenz, P.; Rajagopalan, R. *Principles of Colloid and Surface Chemistry*, 3rd ed.; Merce Dekker, Inc.: New York, New York, 1997.
- [11] Langmuir, I. The Adsorption of Gases on Plane Surfaces of Glass, Mica and Platinum. *J. Am. Chem. Soc.* **1918**, *40*, 1361–1403.
- [12] Clark, A. *The Theory of Adsorption and Catalysis*; Academic Press, Inc.: New York, New York, 1970.
- [13] Liu, Y. Is the Free Energy Change of Adsorption Correctly Calculated? *J. Chem. Eng. Data* **2009**, *54*, 1981–1985.
- [14] Milonjić, S. K. A consideration of the correct calculation of thermodynamic parameters of adsorption. *J. Serb. Chem. Soc.* **2007**, *72*, 1363–1367.
- [15] Rojas, O. J. *Cellulose Chemistry and Properties: Fibers, Nanocelluloses and Advanced Materials*; Springer International Publishing: Cham, Heidelberg, New York, Dordrecht, London, 2016; p 314.
- [16] Li, Y.; Hou, Y.; Zou, Y. Microwave assisted fabrication of nano-ZnO assembled cotton fibers with excellent UV blocking property and water-wash durability. *Fibers Polym.* **2012**, *13*, 185–190.
- [17] Kontturi, E.; Tammelin, T.; Osterberg, M. Cellulose–model films and the fundamental approach. *Chem. Soc. Rev.* **2006**, *35*, 1287–1304.

- [18] Hoven, T. V.; Ramaswamy, G. N.; Kimmel, L.; Boylston, E. Cotton/kenaf fabrics: a viable natural fabric. *J. Cotton Sci.* **1999**, *3*, 60–70.
- [19] Follain, N. *Amines Grafted Cellulose Materials*; Nova Science Publishers: New York, New York, 2010.
- [20] Voncina, B.; Le Marechal, A. M. Grafting of cotton with β -cyclodextrin via poly(carboxylic acid). *J. Appl. Polym. Sci.* **2005**, *96*, 1323–1328.
- [21] Martel, B.; Morcellet, M.; Ruffin, D.; Vinet, F.; Weltrowski, M. Capture and controlled release of fragrances by CD finished textiles. *J. Inclusion Phenom.* **2002**, *44*, 439–442.
- [22] Al-Kahlout, A. ZnO nanoparticles and porous coatings for dye-sensitized solar cell application: Photoelectrochemical characterization. *Thin Solid Films* **2012**, *520*, 1814–1820.
- [23] McMurry, J. *Organic Chemistry*, 4th ed.; Brooks/Cole: Pacific Grove, Ca, Chapter Carboxylic Acid Derivatives and Nucleophilic Acyl Substitution Reactions, p 843.
- [24] Bevington, P. R.; Robinson, D. K. *Data Reduction and Error Analysis for the Physical Sciences*, 3rd ed.; McGraw-Hill, Inc.: New York, NY, 2003.